Supersaturation Fluctuations in Cirrus Clouds Driven by Colored Noise

B. KÄRCHER

Deutsches Zentrum für Luft- und Raumfahrt, Institut für Physik der Atmosphäre, Oberpfaffenhofen, Wessling, Germany

(Manuscript received and in final form 1 June 2011)

ABSTRACT

Fundamental properties of ice supersaturation variability in cirrus clouds are studied by means of an idealized probabilistic model. Damped supersaturation fluctuations are assumed to be exponentially correlated in time, statistically stationary, and normally distributed. The damping process is tied to the ability of the ice crystals to scavenge water vapor. The temporal evolution of supersaturation separates into an early ballistic and a late asymptotic regime. The latter allows for a stationary solution for the probability distribution of supersaturation in the presence of cloud ice and corresponds to a diffusive solution in cloud-free conditions. Low ice crystal number densities, small ice crystal sizes, short supersaturation correlation times, and large fluctuation intensities favor the spreading of cirrus ice crystal sizes, especially in conditions conducive to sublimation. Otherwise, size spreading of ice crystals is hampered by ice-induced damping of supersaturation fluctuations. The spreading of the probability distributions of ice supersaturation for very weak damping may lead to an increase of cirrus fractional coverage, as parameterized in large-scale atmospheric models, even for small mean supersaturations.

1. Introduction

Cirrus clouds may be defined as pure ice clouds forming below a temperature of about 235 K above an altitude of about 7 km (Heintzenberg and Charlson 2009). Cirrus formation and evolution are largely controlled by the development and magnitude of the relative humidity over ice, or supersaturation.[1] Similar to most other atmospheric variables, supersaturation exhibits variability across a wide range of temporal and spatial scales and a number of physical processes contribute to this variability. The lack of understanding of statistical properties of upper tropospheric supersaturation fluctuations is caused in part by the difficulty of measuring relative humidity accurately at high altitudes. Hence, the conditions during ice nucleation (a phase transition that is an extremely sensitive function of supersaturation) and during ice crystal growth (the rate of which is proportional to supersaturation) are difficult to determine. Therefore, key processes controlling cirrus formation and evolution remain uncertain.

In view of the importance of supersaturation and its variability for understanding the physics of clouds and their representation in global models (Siebesma et al. 2009) and in a wider sense for understanding climate change (Pierrehumbert et al. 2007), it is important to raise fundamental issues about this subject. A treatment of atmospheric supersaturation on the molecular level is not feasible, suggesting that a probabilistic description of supersaturation fluctuations is more appropriate. In the case of warm, liquid-water-containing clouds, this area of research has been called stochastic condensation. Much effort has been focused on the broadening of cumulus cloud droplet size distributions in the presence of turbulent supersaturation because of its importance for precipitation formation (Shaw 2003). The present study is a first attempt to approach the issue of ice supersaturation variability for cold cirrus clouds, which experience different dynamical forcing mechanisms and are microphysically different from warm clouds.

Fluctuations in supersaturation relevant to cirrus clouds may occur on the microscale (centimeters) and the lower mesoscale (a few tens of kilometers), up to planetary scales (thousands of kilometers). It is conceivable that turbulence is less significant in affecting supersaturation variability at cirrus levels than in the planetary boundary layer owing to the relatively low turbulence kinetic energies in the upper troposphere. The energy contained in the fluctuations is dissipated

[1] We use the term *supersaturation* to denote conditions in which ice crystals either grow or sublimate.

Corresponding author address: Bernd Kärcher, Deutsches Zentrum für Luft- und Raumfahrt, Institut für Physik der Atmosphäre, Oberpfaffenhofen, Wessling 82234, Germany.
E-mail: bernd.kaercher@dlr.de

DOI: 10.1175/JAS-D-11-0151.1

by molecular diffusion and heat conduction on the microscale. Fluctuations on the mesoscale originate from gravity waves and turbulence (Lilly 1983). It is often difficult to untangle their atmospheric signatures. Measurements revealed convectively driven cirrus-generating cells on scales of about 1 km (Heymsfield 1975) and the existence of ice formation regions with extensions between 15 and 100 km, depending on cirrus cloud type (Sassen et al. 1989). Aircraft measurements further revealed that mesoscale vertical wind fluctuations strongly impact the nucleation of ice in cirrus clouds (Kärcher and Ström 2003). Dynamical processes on larger spatial scales and on long time scales set the mean synoptic conditions in which cirrus form (Haag and Kärcher 2004).

Clouds and their impact on radiation and climate are often studied with a hierarchy of numerical models. The magnitudes and properties of fluctuating atmospheric variables are scale dependent and so are the magnitudes of averaged (e.g., model grid mean) quantities. The coarser a model's spatial resolution, the more important it is to account for unresolved variability in the parameterization of cloud physical processes. Current global climate models employ horizontal resolutions of 100 km or more. Such models are not capable of resolving single clouds or cloud systems and apply in their cloud schemes microphysical relationships based on resolved (grid scale) variables, often without consideration of subgrid-scale variability. The results presented in this study might help explore implications of ice supersaturation variability for nucleation and growth of cirrus ice crystals and spur new ideas of how to improve ice cloud parameterizations in large-scale models.

We present an idealized stochastic model for supersaturation fluctuations (section 2) and study the salient features of its solution (section 3). As first applications, we examine the connection between supersaturation variability and growth of ice crystals by water uptake and explore the consequences of supersaturation variability for the ubiquitous homogeneous ice formation process in cirrus conditions (section 4). We make no attempt to study the impact of supersaturation fluctuations on ice nucleation in detail. Section 5 summarizes our main findings.

2. Stochastic model

The probabilistic concept developed here describes the supersaturation variability in a Lagrangian air parcel containing cirrus ice crystals (Fig. 1). The physical variables distributed in the parcel volume are considered to be spatially homogeneous. The vapor–ice particle system is characterized by a constant ice crystal number density and mean size, and a mean ice supersaturation. We regard the cloudy air parcel as a subsystem immersed in a larger-scale atmospheric flow. We develop and examine a general theoretical framework rather than characterizing the sources of the fluctuations, waves, and turbulence in detail.

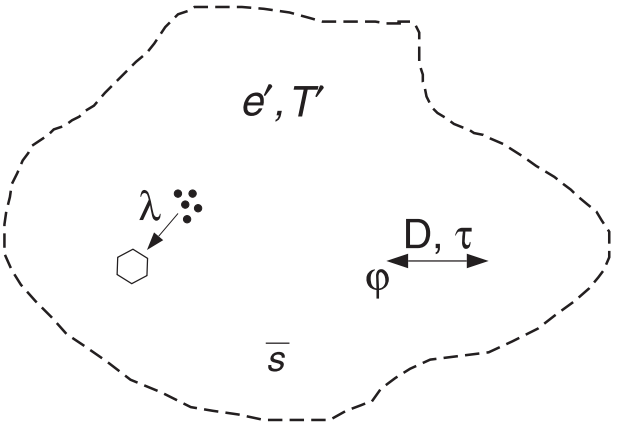

FIG. 1. Factors affecting ice supersaturation in a cloudy air parcel. Rapid fluctuations φ around the mean ice supersaturation $\overline{s}$ are driven by perturbations (noise) of the temperature T' and the water vapor partial pressure e'. The fluctuations are statistically stationary and exponentially correlated with a characteristic time τ and are damped by the uptake of water molecules on the surfaces of ice crystals on the microphysical time scale $1/\lambda$. The noise intensity D scales in proportion to the cloud-free fluctuation variance.

The air parcel is subject to perturbations (noise) of its temperature and/or water vapor partial pressure, both inducing fluctuations of the supersaturation. The noise causes a jitter of the supersaturation, which is damped by diffusional uptake of water vapor on the ice crystal surfaces. This uptake process (depositional growth) is described by a microphysical damping rate. We assume that the temporal fluctuations are exponentially correlated and statistically stationary. We allow for arbitrarily long noise-induced supersaturation correlation times. This type of noise is referred to as colored noise because the spectral density of the fluctuations is frequency dependent. (For white noise, the spectral density is constant, which requires an extremely small, or effectively zero, correlation time.)

To describe the evolution of supersaturation we split the total supersaturation s into components describing the mean $\overline{s}$ and fluctuations around the mean $\varphi: s = \overline{s} + \varphi$. The fluctuations are assumed to evolve on shorter temporal (and spatial) scales than the mean value. For instance, $\overline{s}$ may be determined by large-scale background forcings and long-time correlation processes. Damping processes inside cirrus clouds may cause $\overline{s}$ to approach thermodynamic equilibrium. Here, it is only

necessary to view $\bar{s}$ as an externally given parameter and to consider that a sufficiently large number of air parcels exist within a given volume of air, leading to a well-defined mean value.

The stochastic differential (Langevin) equation

$$\frac{d\varphi}{dt} = -\lambda\varphi + \epsilon(t) \tag{1}$$

contains the most essential elements, damping and forcing, determining the evolution of supersaturation fluctuations in a cloudy air parcel versus time t. The damping rate λ reflects the tendency to restore $\bar{s}$. The random forcings ϵ are characterized by a statistically stationary statistic with zero mean and exponential correlation:

$$\langle\epsilon\rangle = 0, \quad \langle\epsilon(t)\epsilon(t_\star)\rangle = \frac{D}{\tau}\exp\left(-\frac{|t - t_\star|}{\tau}\right); \tag{2}$$

the angle brackets indicate an expectation value, D is a measure of the intensity of the fluctuations (noise strength), and τ is the Lagrangian supersaturation correlation time (noise color). The white noise limit may be recovered by decreasing $\tau \to 0$ and leaving D constant, in which case the covariance from Eq. (2) reverts to $2D\delta(t - t_\star)$. Spatial correlations of supersaturation are not considered.

The damping rate employed here follows from the diffusion equation for water vapor in air (e.g., Twomey 1977):

$$\lambda \equiv t_d^{-1} = 4\pi D_v n\bar{r}, \tag{3}$$

where D_v is the gas diffusion coefficient of water molecules, n is the ice crystal number concentration, and $\bar{r}$ is the corresponding ice particle radius averaged over a size distribution, assuming irregularly shaped ice crystals to be spherical with radii r of volume-equivalent spheres. Furthermore, t_d is the damping time. Equation (3) is related to the diffusive (Maxwellian) flux of water molecules governing the growth of ice crystals by uptake of water molecules. This flux is reasonably accurate for cirrus ice crystals in the size range below a few 100 μm. Other damping processes could be accounted for by using different expressions for λ.

Ice crystal properties vary strongly inside a cirrus cloud. Application of the model requires conditions in the air parcel which are reasonably homogeneous in terms of λ and in which τ is approximately constant.

In nature, inhomogeneities in φ fields could arise between different temperature and/or water vapor concentrations around different ice particles. Over a distance equal to the mean interparticle distance $R = 0.554n^{-1/3}$ (Chandrasekhar 1943) associated spatial gradients will be removed by molecular diffusion of vapor and heat on time scales $t_v \simeq R^2/D_v$. As a consequence, spatial correlations of supersaturation fluctuations remain for distances exceeding R. Typical ranges are $R \approx 0.5$–5 cm and $t_v \approx 0.3$–30 s for $n = 0.001$–1 cm^{-3}. Furthermore, for fixed cloud parameters, the model can be applied up to times $t_m \simeq (d^2/\epsilon_d)^{-1/3}$ over which turbulent diffusion causes full mixing of the air parcel with its (cloudy) environment. Using a parcel dimension $d = 100$ m and energy dissipation rates in cirrus $\epsilon_d \approx 10^{-6}$–$10^{-3}$ m^2 s^{-3} (Quante and Starr 2002), we estimate $t_m \approx 5$–35 min as a conceivable range of air parcel lifetimes against turbulent mixing inside cirrus. Longer t_m values are possible in cloud layers that are less affected by turbulence (e.g., perturbed purely by wave-induced motions). Therefore, t_m lies within the range of cloud-averaged damping times $t_d \approx 1$–100 min, estimated from Eq. (3) using $n = 1$ cm^{-3} and $\bar{r} = 25$ μm for mature midlatitude cirrus, and $n = 0.01$ cm^{-3} and $\bar{r} = 5$ μm for thin, very cold tropical tropopause cirrus. We further note that ice crystals with maximum dimensions less than 100 μm have terminal fall speeds less than 0.5 m s^{-1}, so the assumption of neglecting changes in λ due to sedimentation is accurate in the case of small ice crystals. If the air parcel contains larger ice crystals, λ may change over the time scale t_m because of sedimentation losses. In addition, sedimentation removes moisture affecting the evolution of supersaturation. On the other hand, growth of ice particles due to uptake of water molecules may change λ faster than sedimentation.

Insofar as the supersaturation fluctuations represent the cumulative effect of a large number of weakly coupled perturbations, we can invoke the central limit theorem and treat the probability distribution of the fluctuations P as Gaussian, in which case Eqs. (1) and (2) can be solved analytically (Benkert et al. 1990):

$$P(\varphi, t) = \frac{1}{\sqrt{2\pi\sigma_\varphi^2}}\exp\left[-\frac{(\varphi - \varphi_0 e^{-\lambda t})^2}{2\sigma_\varphi^2}\right], \tag{4}$$

with the variance

$$\sigma_\varphi^2(t;\lambda,\tau) = \frac{D\tau}{(\lambda\tau)^2 - 1}\left[\frac{(\lambda\tau - 1) + (\lambda\tau + 1)e^{-2\lambda t}}{\lambda\tau} - 2e^{-(\lambda\tau+1)t/\tau}\right]. \tag{5}$$

Nonzero initial fluctuations φ_0 are damped over the time scale $1/\lambda$. In the case $\lambda\tau = 1$, the variance is given by

$$\sigma_\varphi^2(t;\lambda\tau \to 1) = \frac{D\tau}{2}\left[1 - \left(1 + 2\frac{t}{\tau}\right)e^{-2t/\tau}\right]. \tag{6}$$

Colored noise allows for arbitrary $\tau > 0$ (e.g., similar to the time scales of the perturbations that drive the stochastic dynamics of the vapor–ice system in the air parcel). While λ is fixed once $n\bar{r}$ is known, τ is an open parameter that needs to be constrained by observations or more detailed models.

3. Discussion

We discuss two distinct regimes of the solution presented in section 2. In the early ballistic regime, subsequent fluctuations are rare and mostly occur in the same direction, leading to a rapid broadening of the probability distribution of supersaturation fluctuations. The asymptotic regime separates into a stationary and nonstationary case. In the asymptotic stationary regime, further broadening of the distribution is suppressed by the ice-induced damping. Without damping, a stationary solution is not possible, and the asymptotic solution corresponds to a random walk problem, in which the supersaturation perturbations change their sign very often and the probability distribution broadens diffusively. The undamped limit describes the evolution of ice supersaturation in cloud-free conditions.

The temporal evolution of the scaled variance $\sigma_\varphi^2/D\tau$ is shown in Fig. 2. The time t_∞ (also shown) separates the ballistic and asymptotic regimes:

$$t_\infty = \begin{cases} \max\left[\dfrac{1}{2\lambda}, \dfrac{\tau}{\lambda\tau + 1}\right]: & \lambda > 0 \\ \tau : & \lambda = 0 \end{cases}. \tag{7}$$

Stationary solutions σ_∞^2 reached after t_∞, are only possible in the presence of damping:

$$\sigma_\varphi^2(\lambda > 0;\quad t \gg t_\infty) \equiv \sigma_\infty^2 \to \frac{D/\lambda}{\lambda\tau + 1}. \tag{8}$$

The undamped limit is given by

$$\sigma_\varphi^2(\lambda \to 0) = 2D\tau(e^{-t/\tau} + t/\tau - 1);\quad 2D\tau \equiv \sigma_{\rm cf}^2, \tag{9}$$

representing a Gaussian stochastic process with an exponential correlation. Equation (9) corresponds to a pure diffusion problem in the asymptotic regime: $\sigma_\varphi^2(\lambda \to 0; t \gg t_\infty) = 2Dt$, in which the fluctuation amplitude (standard deviation) exhibits a square-root dependence on time: $\sigma_\varphi \propto \sqrt{t}$. Equation (9) is used along with dimensional considerations to constrain the noise strength D accounting for the intensity of external perturbations, as there is no microscopic theory from which D could be inferred. Setting $2D\tau$ constant and equal to the variance of the supersaturation fluctuations in cloud-free conditions

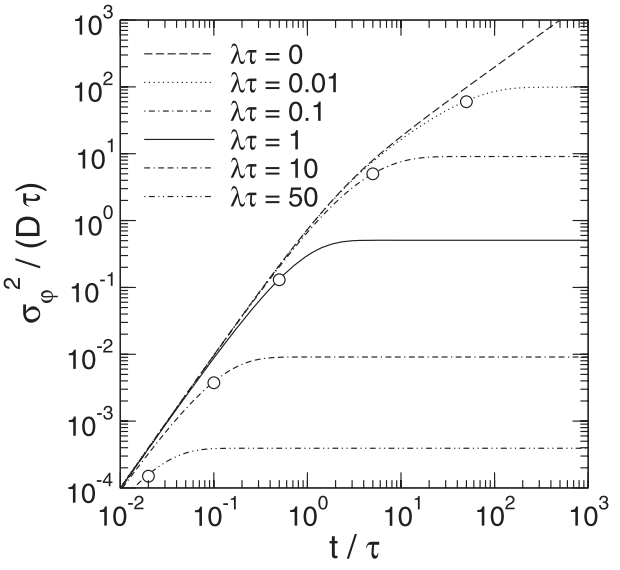

FIG. 2. Normalized variance of supersaturation fluctuations vs time t scaled by the supersaturation correlation time τ. The damping rate is λ, with $\lambda = 0$ describing the cloud-free limit. Stationary solutions are realized for $\lambda > 0$ and are reached after t_∞/τ (circles). The dimensionless damping parameter $\lambda\tau$ describes the stochastic dynamics of supersaturation fluctuations.

$\sigma_{\rm cf}^2$ fixes the noise strength, or supersaturation diffusion coefficient: $D = \sigma_{\rm cf}^2/2\tau$. In this case, we can no longer perform the white noise limit formally in Eq. (2), since D and τ cannot be varied independently. The model proposed here for supersaturation fluctuations may be viewed as a modification of the white noise process describing Brownian motion (Einstein 1905), allowing for perturbations with arbitrary correlation time (Uhlenbeck and Ornstein 1930) and a diffusion coefficient independent of the damping rate.

In the ballistic regime, we find in the undamped limit that

$$\sigma_\varphi^2(\lambda \to 0; t \ll t_\infty) = D\tau(t/\tau)^2 \tag{10}$$

(i.e., $\sigma_\varphi \propto t$; the amplitude increases significantly faster than in the diffusion regime). For very weak damping ($\lambda \ll 1$), σ_φ^2 is not sensitive to changes of λ in the ballistic regime (see Fig. 2). On the contrary, σ_∞^2 decreases rapidly with increasing λ.

Rapid temperature fluctuations induced by a spectrum of small-scale gravity waves are known to cause significant variability in supersaturation in cloud-free conditions (Hoyle et al. 2005). We seek a relationship between $\sigma_{\rm cf}$ and the temperature fluctuation amplitudes T'. Aircraft data taken away from convection or mountainous regions hint at mean mesoscale vertical displacements of air parcels in the range $L \approx$ 10–140 m at an altitude of about 11 km (Gary

2006), depending on geographical location, season, and type of underlying terrain. Using $L = 100$ m, then $T' = \Gamma \times L \approx 1$ K with the dry adiabatic lapse rate $\Gamma = 0.01$ K m^{-1}. Ice supersaturation is defined by $s = (e/e_s) - 1$ with the saturation vapor pressure $e_s = 3.4452 \times 10^{10} \exp(-Q/T)$ (Marti and Mauersberger 1993), valid within $170 < T < 250$ K, giving e_s in millibars, and $Q = 6132.9$ K being the latent heat of sublimation in temperature units. Using $T = \overline{T} + T'$ and $e' = 0$, it is easy to show that

$$\sigma_{\rm cf} \simeq s' \equiv \sqrt{(s - \overline{s})^2} = (\overline{s} + 1)\theta \frac{|T'|}{\overline{T}}, \qquad (11)$$

with $\theta = Q/\overline{T}$ and $\overline{s} = \overline{e}/e_s(\overline{T}) - 1$, valid for $\theta|T'|/\overline{T} \ll 1$. Inserting $T' = 1$ K yields $\sigma_{\rm cf} \simeq 0.12$ using $\overline{s} = 0$ and a mean temperature $\overline{T} \simeq 225$ K. (The above range for L implies $\sigma_{\rm cf} \simeq 0.05$–$0.17$.) Additional e-fluctuations uncorrelated with T would increase $\sigma_{\rm cf}$; such an increase is (partly) compensated by adiabatic correlations between e' and T' (Kärcher and Burkhardt 2008).

Aircraft measurements of relative humidity and cirrus properties have been carried out over Southern Chile during the Interhemispheric Differences in Cirrus Properties from Anthropogenic Emissions (INCA) project (Gayet et al. 2006). The appropriately normalized model frequency distribution, using the undamped supersaturation variance from Eq. (9) with $\sigma_{\rm cf} = 0.12$ and $t/\tau = 0.75$, is compared to the INCA statistic taken in cloud-free conditions (Kärcher and Haag 2004) in Fig. 3. This statistic has a local maximum near saturation. The fair agreement between the model distribution and the moistest mode builds confidence in our rough estimate for $\sigma_{\rm cf}$.

The observed statistic does not represent a coherent Lagrangian time series, limiting the ability to compare these data with our model. Nonetheless, the assumption of Gaussian supersaturation fluctuations appears to be a reasonable approximation. The exact form of the probability distribution does not matter if only the low-order moments (especially mean and variance) are important for a specific problem.

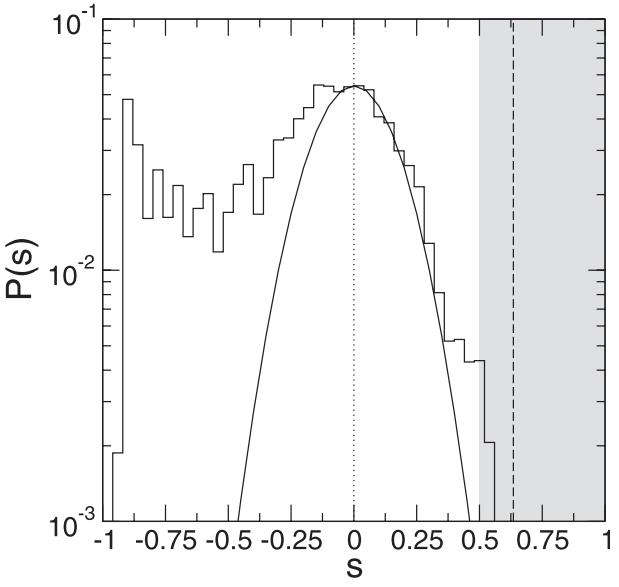

FIG. 3. Probability distribution of cloud-free ice supersaturation from aircraft measurements taken over Punta Arenas (52°–60°S, 70°–85°W) during 4 weeks in March–April 2000 (stepped lines) and frequency distribution from the undamped model solution with $\varphi_0 = 0$, centered at $\overline{s} = 0$ (solid curve). The observations comprise several dry and moist modes. The bin widths roughly correspond to the precision of the in situ measurements. Small ice crystals may have been present in some of the data taken at the highest supersaturations. The model distribution variance was constrained by small-scale temperature fluctuations ($T' = 1$ K), leading to $\sigma_{\rm cf} = 0.12$, and $t/\tau = 0.75$ was used as a parameter to approximate the tail of the moistest mode that was observed. The dotted line at ice saturation separates conditions in which the ice phase is stable ($s > 0$) or unstable ($s < 0$). The dashed line marks water-saturated conditions at $\overline{T} = 225$ K. The gray-shaded area marks the conditions at which ice crystals form by homogeneous aerosol particle freezing, the dominant cirrus formation mechanism during these observations.

4. Atmospheric implications

Supersaturation fluctuations affect the mass growth rate of ice crystals due to uptake of water molecules diffusing through air. As the fluctuations cause positive and negative variations around a mean value, and smaller ice crystals grow faster than larger ones, we expect ice crystal sizes to spread (section 4a). At very low cloud ice number concentrations or in clear air, new ice crystals may be formed once the supersaturation exceeds a threshold value. The portion of the supersaturation distribution exceeding this threshold is related to the probability of cirrus formation (section 4b).

a. Spreading of ice crystal sizes

A spreading factor, measuring the relative size dispersion of an initially monodisperse ice crystal population, is defined as

$$\beta \equiv \frac{r_+ - r_-}{\overline{r}}. \qquad (12)$$

The mean radius $\overline{r}$ and the largest r_+ and smallest radii and r_- attained during fluctuation-induced growth or sublimation, are given by

$$\overline{r} = r_0 \sqrt{1 + \overline{s}\gamma t}, \qquad (13)$$

$$r_\pm = r_0 \sqrt{1 + (\overline{s} \pm \sigma_\infty)\gamma t}, \qquad (14)$$

with the initial radius r_0. They follow from the depositional growth equation for spherical particles (Twomey 1977):

$$\frac{d(r/r_0)^2}{dt} = \gamma(\overline{s} + \varphi). \quad (15)$$

Equation (15) states that dr/dt decreases with increasing radius. To evaluate β, we integrate this growth law using a constant growth rate factor γ and the asymptotic stationary standard deviations $\pm\sigma_\infty$ of the supersaturation fluctuations replacing the actual values φ. This leads to Eqs. (13) and (14). The parameter γ is defined as the inverse of the initial areal growth time scale per unit supersaturation t_g:

$$\gamma \equiv t_g^{-1} = \frac{2\nu D_v}{r_0^2}\frac{e_s}{kT}, \quad (16)$$

evaluated at $T = \overline{T}$. Here, ν is the volume of a water molecule in ice and k is Boltzmann's constant. Typical t_g values range between about 3 s and 30 min for small cirrus ice crystals with $r_0 = 10$ μm and $T = 190$–240 K. The approximations underlying Eqs. (15) and (16) are the same as those underlying the damping factor from Eq. (3).

Figure 4 illustrates that for weak damping and/or short correlation times, cases $\lambda\tau = 0.01$ and 0.1 (upper panel), sizes spread quickly ($\beta > 1$) within the characteristic growth time ($\gamma t < 1$), regardless of the mean supersaturation in the range $[-0.15, 0.15]$ when assuming a cloud-free standard deviation $\sigma_{cf} = 0.1$ (cf. the discussion of Fig. 3). This is because r_- decreases rapidly when ice crystals sublimate. For $\lambda\tau = 1$, damping occurs between $\overline{s} = 0$ and $\overline{s} = 0.15$. Spreading is suppressed very efficiently ($\beta < 0.3$) for $\overline{s} = 0.15$ for all $\lambda\tau$ cases shown. For $\lambda\tau = 10$, efficient size spreading occurs only when all ice crystals sublimate in mean conditions ($\overline{s} = -0.15$). We additionally note that higher values, $\lambda\tau > 10$, suppress the spreading for a large range of $\overline{s}$ around ice saturation for the assumed range of σ_{cf} values.

b. Onset of cirrus formation

The area of the distribution of supersaturation above the ice formation threshold s_{thr} may be interpreted as an increase in cirrus cloud fraction (spatial coverage) (Kärcher and Burkhardt 2008). For very weak damping or in the absence of cloud particles, $P(s, t)$ broadens over a long time because t_∞ becomes large. Therefore, cirrus formation can be triggered by variability in s, even if the ensemble mean is well below the ice nucleation threshold. This is an essential aspect in any parameterization of cloud formation in large-scale atmospheric models incapable of resolving individual clouds.

The increase in cirrus cloud fraction from our model (using $\varphi_0 = 0$) is given by

$$\eta \equiv P(s \geq s_{thr}, t) = \frac{1}{\sqrt{2\pi}\sigma_\varphi}\int_{s_{thr}}^{\infty} \exp\left[-\frac{(s-\overline{s})^2}{2\sigma_\varphi^2}\right] ds, \quad (17)$$

which leads to the solution

$$\eta = \frac{1}{2}[1 - \mathrm{erf}(X)], \quad X = \frac{s_{thr} - \overline{s}}{\sqrt{2}\sigma_\varphi}, \quad (18)$$

with the error function erf$(\cdot)$. Results using the undamped variance, Eq. (9), are shown in Fig. 5 for $s_{thr} = 0.5$, representing upper tropospheric homogeneous freezing conditions (Koop et al. 2000).

Generally, η increases with time as the distribution broadens (σ_φ increases) and η rises earlier for larger $\overline{s}$ and σ_{cf}, in which case the distribution tail is closer to s_{thr}. It does not approach unity because the mean supersaturation lies below the formation threshold. It is remarkable that cirrus coverage may increase even in mean sublimation conditions ($\overline{s} = -0.15$), although only in the asymptotic diffusion regime (i.e., after long times or for short correlation times; $t/\tau > 1$–10). Damping mechanisms in cloud-free air that are not considered here may modify this result.

If variability in supersaturation solely arises from temperature fluctuations with a symmetric probability distribution, then the resulting distribution of supersaturation is skewed toward high s values. This is caused by the Clausius–Clapeyron relationship underlying $e_s(T)$. The term $P(s)$ has been explicitly derived for Gaussian temperature distributions (Kärcher and Haag 2004), in which case the skewness in $P(s)$ becomes negligible for fluctuation amplitudes $T' < 0.5$ K at cold temperatures. Skewness in $P(s, t)$ would affect the shape of $\eta(t)$. Nonetheless, our general conclusions drawn from Fig. 5 would not change.

Turbulence created inside cirrus clouds can be another source of supersaturation variability. Latent heating–induced turbulence energy dissipation rates of about 10^{-4} m^2 s^{-3} have been simulated to induce peak updraft speeds of 35 cm s^{-1} in localized cells of a deep (vertical extension 2–4 km), optically thick (solar optical depth 2–3) stratiform cirrus cloud (Sölch and Kärcher 2011). Such updrafts, and the associated cooling rates ($\sim$K h^{-1}), are comparable to those created during cirrus initiation by external gravity wave sources. Radiative heating or cooling tendencies are smaller ($\sim$K day^{-1}) and therefore affect supersaturation at longer time scales. On the one hand, our model assumes that the statistical properties of all interacting noise sources, as expressed in Eq. (2), do

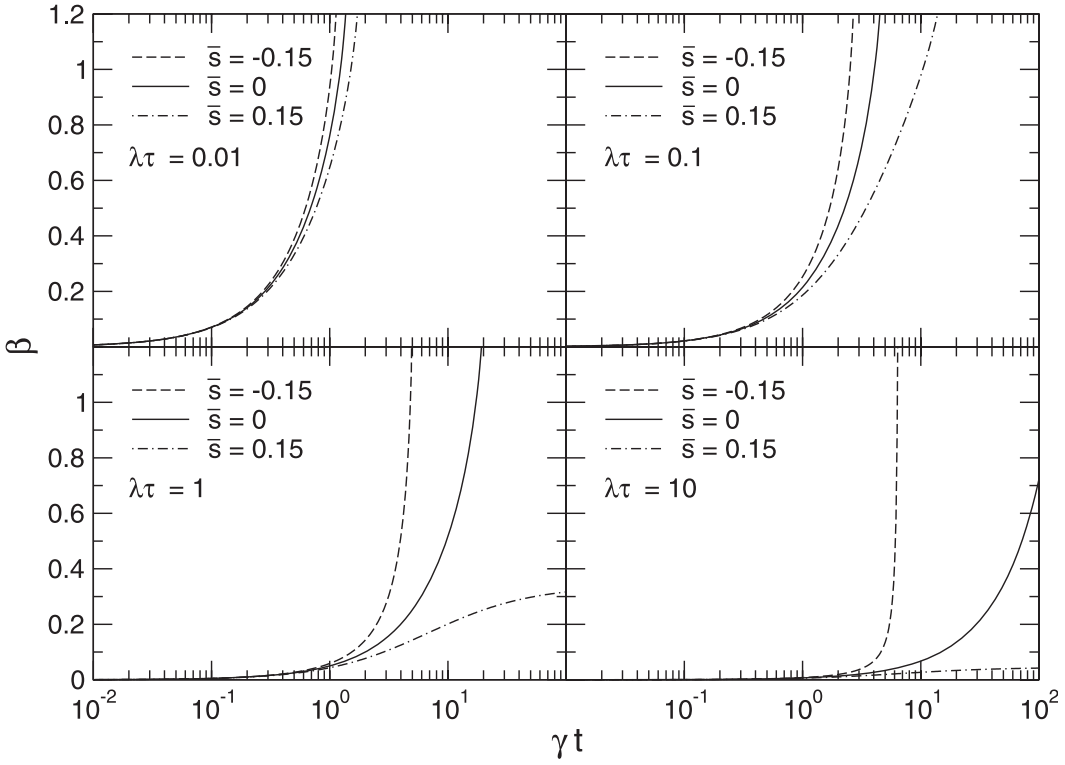

FIG. 4. Broadening factor for initially monodisperse ice crystals as a function of the scaled depositional growth time γt of ice crystals, for various combinations of the dimensionless damping parameter $\lambda\tau$ and mean supersaturation $\bar{s}$. Here, γ denotes the inverse growth time scale. The mean equilibrium state ($\bar{s} = 0$, i.e., no mean ice particle growth or sublimation) is included. The broadening factor is a measure for the spreading of ice crystal sizes during depositional growth and has been estimated using the asymptotic stationary variances together with a cloud-free fluctuation amplitude $\sigma_{cf} = 0.1$.

not depend on λ. On the other hand, the turbulence intensity diminishes with smaller cloud optical depth and lower temperature.

5. Summary and conclusions

We have introduced and discussed a probabilistic conceptual framework describing small-scale temporal fluctuations of ice supersaturation in cirrus clouds in the framework of a Lagrangian parcel model. The ensemble mean supersaturation is kept constant over the short time scales relevant to our study. The model is based on an exponential temporal correlation of normally distributed fluctuations with a nonzero, finite correlation time. The random fluctuations are damped by uptake of water vapor on preexisting ice crystals. The associated damping rate is not related to the fluctuation sources that are treated as colored noise. The damped fluctuation intensity scales in proportion to the variance of supersaturation in cloud-free conditions. A typical range of the cloud-free supersaturation variance has been estimated based on observed properties of mesoscale temperature fluctuations.

The model is deliberately kept very general, including only the most essential factors controlling the temporal evolution of supersaturation in cirrus, and ignores possible spatial correlations. Exponential correlations and Gaussian probability distributions are often used to approximate the very complex behavior of real physical systems, enabling a rigorous analytical description of fluctuating variables. We therefore hope that the fundamental behavior and basic trends of supersaturation variability in cirrus are correctly described as a function of the key controlling parameters (i.e., fluctuation intensity, Lagrangian correlation time, and microphysical damping rate).

Random fluctuations lead to an increase of the variance of the supersaturation probability distribution over time. We have described a ballistic regime, realized for large correlation times, in which the variance increases rapidly. The asymptotic limit is realized for small correlation times. In this regime, two solutions can be attained depending on the damping strength: a stationary solution with constant variance or a time-dependent diffusion solution in which the variance rises at a slower

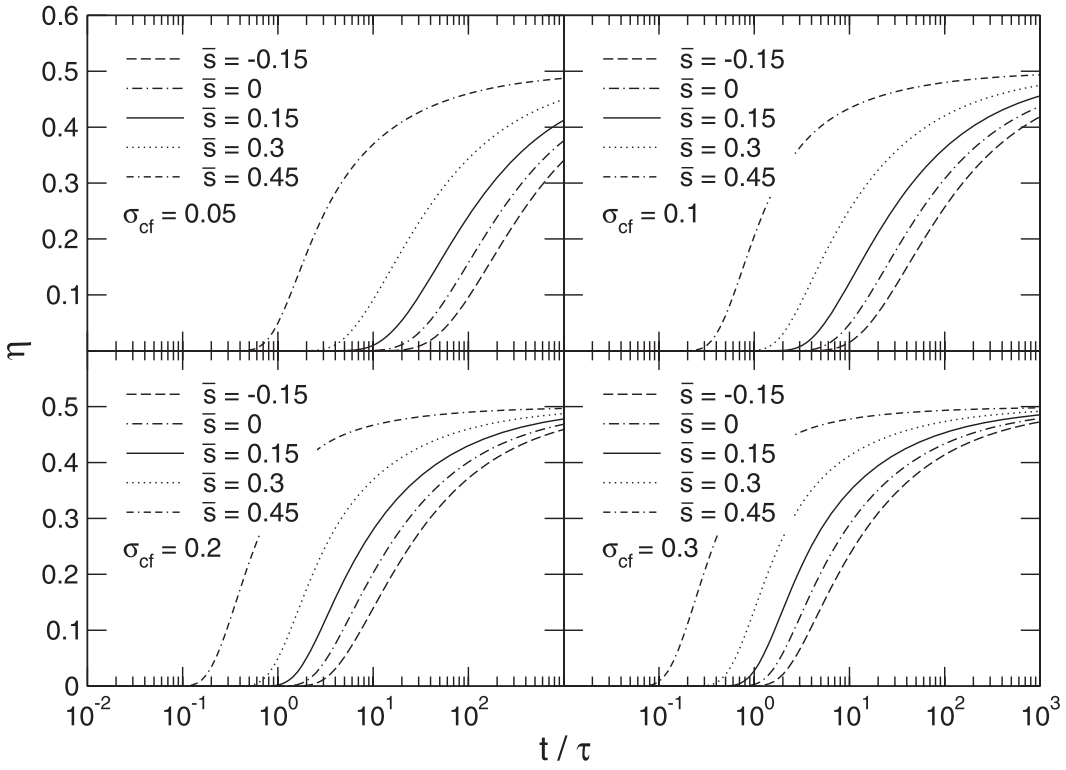

FIG. 5. Fractions of the distribution of supersaturation above the homogeneous aerosol freezing threshold $s_{thr} = 0.5$ as a function of time t scaled by the supersaturation correlation time τ for various combinations of the cloud-free ($\lambda = 0$) supersaturation fluctuation amplitude σ_{cf} and ensemble mean supersaturation $\bar{s}$. The fractions increase because of ballistic and diffusional broadening of the supersaturation distribution in an initially cloud-free environment, and are equivalent to increases in cirrus cloud coverage as simulated with large-scale models using coarse spatial grids. For such cases, $\bar{s}$ may represent the grid-mean supersaturation and φ may account for the unresolved fluctuations.

pace than in the ballistic case. Whereas the microphysical damping rate is known for given cloud parameters, we postpone the quantification of the Lagrangian supersaturation correlation time.

We have investigated fundamental consequences of supersaturation variability for the depositional growth of ice crystals and for cirrus formation via homogeneous freezing of aerosol particles. Low ice crystal number densities, small mean ice crystal sizes, short correlation times, and large fluctuation amplitudes lead to efficient size spreading, especially when ice crystals sublimate. Otherwise, we expect the size spreading to be efficiently suppressed. As the fluctuation variance increases with time in cloud-free conditions (disregarding additional damping mechanisms), cirrus coverage can increase even for mean supersaturations below the ice crystal formation limit (i.e., those representing averages over grid boxes of large-scale models). Fractional coverage is a determinant of cloud radiative forcing as calculated in such models.

Further applications of the theory will likely require the use of more complex (numerical) models, for which our model results may provide useful theoretical guidance. Observational data on Lagrangian supersaturation correlation properties from high-resolution time series of relative humidity will also be needed to unravel the sources and characteristics of supersaturation fluctuations inside and outside of cirrus clouds and to estimate the correlation time and the cloud-free supersaturation variance.

Acknowledgments. Discussions with George Craig (University of Munich, Department of Meteorology), Wolfgang Schleich (University of Ulm, Institute for Quantum Physics), and Ulrike Burkhardt and Ingo Sölch (DLR Oberpfaffenhofen, Institute for Atmospheric Physics) have been helpful in writing this paper.

REFERENCES

Benkert, C., M. O. Scully, A. A. Rangwala, and W. Schleich, 1990: Quantum-noise suppression in lasers via memory-correlation effects. *Phys. Rev.*, **42A,** 1503–1514.

Chandrasekhar, S., 1943: Stochastic problems in physics and astronomy. *Rev. Mod. Phys.,* **15,** 1–89.

Einstein, A., 1905: Über die von der molekularkinetischen Theorie der Wärme geforderte Bewegung von in ruhenden Flüssigkeiten suspendierten Teilchen. *Ann. Phys.,* **322,** 549–560.

Gary, B., 2006: Mesoscale temperature fluctuations in the stratosphere. *Atmos. Chem. Phys.,* **6,** 4577–4589.

Gayet, J.-F., and Coauthors, 2006: Microphysical and optical properties of midlatitude cirrus clouds observed in the Southern Hemisphere during INCA. *Quart. J. Roy. Meteor. Soc.,* **132,** 2719–2748.

Haag, W., and B. Kärcher, 2004: The impact of aerosols and gravity waves on cirrus clouds at midlatitudes. *J. Geophys. Res.,* **109,** D12202, doi:10.1029/2004JD004579.

Heintzenberg, J., and R. J. Charlson, 2009: Introduction. *Clouds in the Perturbed Climate System: Their Relationship to Energy Balance, Atmospheric Dynamics, and Precipitation.* J. Heintzenberg and R. J. Charlson, Eds., MIT Press, 1–15.

Heymsfield, A. J., 1975: Cirrus uncinus generating cells and the evolution of cirriform clouds. Part II: The structure and circulation of the cirrus uncinus generating head. *J. Atmos. Sci.,* **4,** 809–819.

Hoyle, C. R., B. P. Luo, and T. Peter, 2005: The origin of high ice crystal number densities in cirrus clouds. *J. Atmos. Sci.,* **62,** 2568–2579.

Kärcher, B., and J. Ström, 2003: The roles of dynamical variability and aerosols in cirrus cloud formation. *Atmos. Chem. Phys.,* **3,** 823–838.

——, and W. Haag, 2004: Factors controlling upper tropospheric relative humidity. *Ann. Geophys.,* **22,** 705–715.

——, and U. Burkhardt, 2008: A cirrus cloud scheme for general circulation models. *Quart. J. Roy. Meteor. Soc.,* **134,** 1439–1461.

Koop, T., B. P. Luo, A. Tsias, and T. Peter, 2000: Water activity as the determinant for homogeneous ice nucleation in aqueous solutions. *Nature,* **406,** 611–614.

Lilly, D. K., 1983: Stratified turbulence and the mesoscale variability of the atmosphere. *J. Atmos. Sci.,* **40,** 749–761.

Marti, J., and K. Mauersberger, 1993: A survey and new measurements of ice vapor pressure at temperatures between 170 and 250 K. *Geophys. Res. Lett.,* **20,** 363–366.

Pierrehumbert, R. T., H. Brogniez, and R. Roca, 2007: On the relative humidity of the atmosphere. *The Global Circulation of the Atmosphere*, T. Schneider and A. Sobel, Eds., Princeton University Press, 143–185.

Quante, M., and D. O. Starr, 2002: Dynamical processes in cirrus clouds. *Cirrus,* D. K. Lynch et al., Eds., Oxford University Press, 346–374.

Sassen, K., D. O. Starr, and T. Uttal, 1989: Mesoscale and microscale structure of cirrus clouds: Three case studies. *J. Atmos. Sci.,* **46,** 371–396.

Shaw, R. A., 2003: Particle-turbulence interactions in atmospheric clouds. *Annu. Rev. Fluid Mech.,* **35,** 183–227.

Siebesma, A. P., and Coauthors, 2009: Cloud-controlling factors. *Clouds in the Perturbed Climate System: Their Relationship to Energy Balance, Atmospheric Dynamics, and Precipitation,* J. Heintzenberg and R. J. Charlson, Eds., MIT Press, 269–290.

Sölch, I., and B. Kärcher, 2011: Process-oriented large eddy simulations of a midlatitude cirrus cloud system based on observations. *Quart. J. Roy. Meteor. Soc.,* **137,** 374–393.

Twomey, S., 1977: *Atmospheric Aerosols*. Developments in Atmospheric Sciences Series, Vol. 7, Elsevier, 302 pp.

Uhlenbeck, G. E., and L. S. Ornstein, 1930: On the theory of Brownian motion. *Phys. Rev.,* **36,** 823–841.